
Fully Test-time Adaptation by Entropy Minimization

Dequan Wang*
BAIR, UC Berkeley
dqwang@cs.berkeley.edu

Evan Shelhamer*
Adobe Research
shelhamer@adobe.com

Shaoteng Liu
BAIR, UC Berkeley
shaoteng@berkeley.edu

Bruno Olshausen
BAIR & Redwood Center, UC Berkeley
baolshausen@berkeley.edu

Trevor Darrell
BAIR, UC Berkeley
trevor@cs.berkeley.edu

Abstract

Faced with new and different data during testing, a model must adapt itself. We consider the setting of fully test-time adaptation, in which a supervised model confronts unlabeled test data from a different distribution, without the help of its labeled training data. We propose an entropy minimization approach for adaptation: we take the model’s confidence as our objective as measured by the entropy of its predictions. During testing, we adapt the model by modulating its representation with affine transformations to minimize entropy. Our experiments show improved robustness to corruptions for image classification on CIFAR-10/100 and ILSVRC and demonstrate the feasibility of target-only domain adaptation for digit classification on MNIST and SVHN.

1 Introduction

Deep networks can achieve high accuracy on training data and are effective for testing data from the same distribution, as evidenced by tremendous benchmark progress [18, 34, 12]. However, generalization to new and different data is limited [13, 29, 8]. When the training (source) data differ from the testing (target) data, a condition known as *dataset shift* [26], then model accuracy suffers. Models can be sensitive to corruptions, variations, or shifts during testing that were not encountered during training. Nevertheless, it can be necessary to deploy a model in changing conditions on data from different distributions.

We seek to reduce generalization error given only an already trained model and target data. That is, without recourse to the training/source data, as it may no longer be available, or it may be computationally infeasible. This is the condition of a model in deployment, such as on computationally-constrained devices on the “edge” (such as phones or robots [37]), or a model downloaded from a zoo and brought to bear on new data, as is now commonplace. We call this setting fully test-time adaptation.

Fully test-time adaptation has practical motivations. 1. Availability: a model might be distributed without its data, the source data might be protected for privacy concerns, or it might simply be gone. 2. Efficiency: it might not be computationally practical to (re-)process the source data during testing. This is especially true on edge devices, where limits are more strict. 3. Accuracy: a model might not be sufficiently accurate on new data for its purpose.

Fully test-time adaptation is an unsupervised setting, so the model must extract its own supervision. Our objective for test-time optimization is model confidence, as measured by the entropy of the model’s predictions on the test set. For our entropy minimization, we augment the model with an adaptor, which we optimize while keeping the model fixed. The adaptor modulates the model

*Equal contribution.

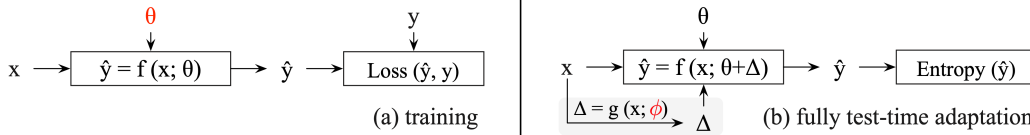


Figure 1: Fully test-time entropy minimization modulates the model $f(x; \theta)$ through an adaptor $g(x; \phi)$ to reduce generalization error on new and different test data. The adaptor maximizes model confidence by minimizing the entropy of model predictions on the test set. Our method does not require any modification of the training of the model f , nor re-training of its parameters θ . Only unlabeled test data is given in this setting—no source data or supervision are available. Red symbols indicate the optimized parameters for each phase.

representation by feature-wise affine transformations, an efficient class of transformations for test-time optimization. The adaptor is optimized purely by entropy minimization of the model predictions during testing. No joint optimization on train and test data is required, and the adaptor never sees training/source data. No re-training or re-architecting of the model is needed.

Our experiments investigate robustness to image corruptions, domain shift for digit recognition, and ablation and oracle analysis. We compare our method to normalization and optimization baselines in the same fully test-time adaptation setting. For reference results given more data and supervision, we also report the accuracies of semi-supervised learning and domain adaptation methods with access to the labeled training data.

Fully test-time adaptation by entropy minimization reduces generalization error for common image corruptions on CIFAR-10/100 and ILSVRC. We show the feasibility of domain adaptation with only target data for digit classification on SVHN and MNIST. We improve on both test-time normalization and self-supervision, even when self-supervision is augmented by joint training on source data. Our method does no harm on a “clean” test set without differences from train. The ablation and oracle experiments support our choice of entropy objective and adaptor architecture.

Our contributions

1. We highlight the setting of fully test-time adaptation, with supervised model and test data alone.
2. We are the first to show the efficacy of entropy as a fully test-time objective, in contrast to its role as a regularizer for a supervised training. This is surprising, in that a supervised model has learned enough during training to adapt itself during testing such that reducing its entropy reduces error.
3. For robustness to corruptions, our method achieves higher accuracy than test-time training by self-supervision, and requires less computation by doing without joint training.
4. For domain adaptation, we show the feasibility of target-only adaptation on a simple digit classification problem, with competitive accuracy to the standard unsupervised domain adaptation setting which requires source and target data.

2 Entropy Minimization via Modulation

In fully test-time adaptation, there is a supervised model f_θ with trained parameters θ and test data $D = x_1, \dots, x_N$. The model must adapt to new and different data during testing without recourse to source data or labeled target data. We adapt the model through test-time optimization to minimize the entropy of predictions by modulating its features. Figure 1 illustrates the proposed method. Fully test-time optimization requires (1) a compatible model, (2) an objective to minimize, and (3) parameters to optimize over.

Model Requirements The model to be adapted must be trained for the supervised task, probabilistic, and differentiable. Supervised training is needed because no supervision is provided during testing, so the model must already be supervised for the task to be done. Probabilistic inference is needed to define a distribution over predictions, and therefore an entropy of the predictions. Differentiability is needed to take the gradient of entropy through the model for iterative optimization during testing.

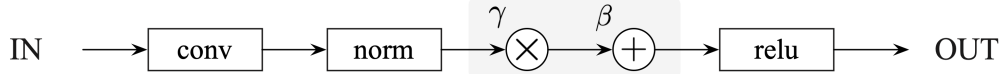


Figure 2: During test-time, we add affine modulation parameters for each channel of the model features chosen for adaptation. The modulation is a channel-wise transformation of the model features, with the scale γ followed by the shift β . These parameters are initialized to one and zero respectively, to set the modulation to the identity and begin adaptation with the original model.

We select off-the-shelf deep image classifiers as representative models for supervised learning with deep networks. These satisfy our three conditions in that they are pre-trained, probabilistic by their predicted softmax distribution over classes, and end-to-end differentiable by construction. Note however that our method is not restricted to softmax classifiers—other compatible probabilistic models include regressors with predictive variance [16] or mixture-of-experts models.

2.1 Entropy Objective

We measure model uncertainty by the Shannon entropy H [32] of the predictions \hat{y} :

$$H(\hat{y}) = - \sum_c p(\hat{y}_c) \log p(\hat{y}_c), \quad (1)$$

where \hat{y}_c denotes the predicted probability of class c . This is a totally unsupervised objective, without the true target y for the task. Nevertheless, the entropy is a function of the task training, as a measure of the model predictions. In this way it is an intrinsic signal for the trained task.

In contrast, auxiliary tasks used for self-supervised optimization are not directly related to the trained task. As such, care is needed to choose an auxiliary task compatible with the domain and task, and a balance must be struck for optimization. For concreteness: examples of these tasks include rotation prediction [9], context prediction [4], and cross-channel auto-encoding [42]. Too much progress on an auxiliary task could interfere with performance on the supervised task, and self-supervised adaptation methods have to limit or mix updates accordingly [36, 35]. Our entropy objective encounters no such difficulties, and our fully test-time optimization helps generalization in either few or many steps.

2.2 Modulation Parameters

Entropy minimization requires a choice of parameters for updating. The model parameters θ are a natural choice, and this is the choice of prior work on entropy minimization in semi-supervised [10] and few-shot [3] learning regimes. However, θ is the only representation of the training/source data in our setting, and altering θ could cause drift from the training data and supervised task. Plus, f can be complicated and θ high dimensional, making optimization too sensitive and time-consuming for test-time usage.

Instead, we augment the model with an adaptor to adjust the model through modulations δ . For our purpose, the adaptor must be simpler than the model in number of parameters and non-linearity. This is appropriate given its role of adjustment, while the model itself is responsible for the task.

Our modulations are affine transformations with scale γ and shift β (see Figure 2). A scale and shift are assigned to each channel k of the model representation chosen for adaptation. Each modulation $\delta_k = \gamma_k, \beta_k$ can be a parameter ϕ , or itself a prediction $\delta_k = g_\phi(x)$. In our experiments we use the direct parameterization of ϕ , as this form of modulation is linear and low dimensional for efficient and stable optimization.

2.3 Algorithm

We minimize the entropy of the model predictions with respect to affine modulation parameters on the test set. We optimize the modulation parameters by stochastic gradient descent with an adaptive optimizer while we simultaneously update the normalization statistics on test data. The optimization shares the same parameters for all test points, unlike the episodic optimization of TTT [36], which independently optimizes each test point.

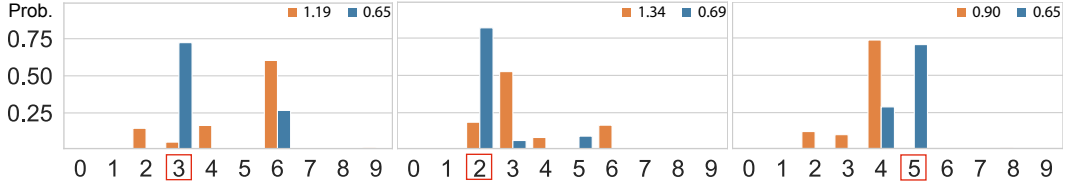


Figure 3: Examples of how fully test-time entropy minimization adapts predictions on corrupted CIFAR-10 (gaussian noise). The class predictions $p(\hat{y}|x)$ before (orange) and after (blue) adaptation show 1) correction in switching to the true class (in red) and 2) entropy reduction (see legend). Our adaptation optimizes over the test set as a whole, yielding correction, while independent optimization of each test point would merely yield more certainty, whether right or wrong.

Initialization We first initialize the modulation parameters $\phi = \{\gamma_{l,k}, \beta_{l,k}\}$ for each model layer l and channel k for adaptation. The γ and β are set to 1 and 0 respectively, so that the modulation is initialized to the identity, preserving the model.

Iteration At each step t , the modulation parameters and normalization statistics are updated. The modulation parameters $\phi^{(t)}$ are updated by the gradient of the prediction entropy $\nabla H(\hat{y})$ to $\phi^{(t+1)}$. The normalization statistics are updated from moving statistics of the training set to the population statistics on the test set.

Termination The simplest and most efficient choice is to optimize for a single epoch. This only necessitates $2\times$ the inference time plus $1\times$ the gradient time per test point vs. the standard $1\times$ inference time of the regular, unadapted model. It is possible to continue optimization for multiple epochs for further improvement. Unlike self-supervised objectives, which may interfere with the supervised task, our entropy objective converges and does no harm with further steps.

Inference Once optimization is complete, we carry out a last pass over the data to make predictions given the learned modulation parameters ϕ and the updated normalization statistics.

3 Experiments

We evaluate our method on corrupted CIFAR-10/100 and ILSVRC and on digit domain adaptation from SVHN to MNIST. Our results on corruption show the effectiveness of fully test-time entropy minimization for improving robustness. Our results on domain adaptation demonstrate the feasibility of cross-domain generalization without access to the source domain, and outperform unsupervised domain adaptation methods that rely on source domain data.

Our method and experiments are implemented on top of the *pycls* library [27, 28] in PyTorch [24]. Our (anonymized) code is included with this submission, and code will be released for publication.

Models For corruption experiments we use a residual network [12] with 26 layers, following [36]. For domain adaptation experiments we use the same network with two different channel width variants (W1 and W4), and a simple LeNet [20] variant from existing works [7, 38, 39]. These architectures are shared by all methods in each experimental condition for fair comparison.

Our networks are equipped with batch normalization [14], and we experiment with its adaptive extension [22] for a strong, optimization-free adaptation baseline.

Datasets We evaluate on standard datasets for image classification and domain adaptation.

For comparison and ablation experiments at an accessible scale we choose CIFAR-10 and CIFAR-100 [19]. These datasets have 10 and 100 classes respectively, a training set of 50,000 images, and a test set of 10,000. For large-scale experiments we choose ILSVRC [31], with 1,000 classes, training set of 1.2 million images, and validation set of 50,000 images.

For digit domain adaptation we choose SVHN [23] and MNIST [20] as source and target domain, respectively. Both datasets have ten classes from the digits 0–9. MNIST consists of binarized

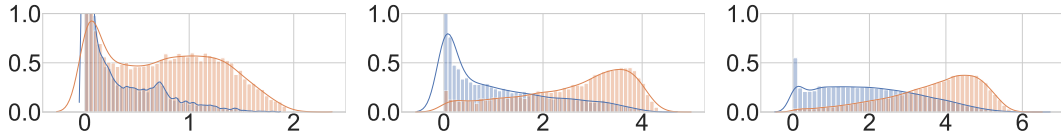


Figure 4: The distribution of prediction entropy on corrupted CIFAR-10, CIFAR-100, and ImageNet (gaussian noise, left-to-right). Before adaptation (orange) entropy spans a large range, while after adaptation (blue) entropy is lower. Our adaptation does indeed reduce the entropy of predictions.

handwritten digits with a training set of 60,000 and test set of 10,000. SVHN consists of color images of house numbers from street views with a training set of 73,257 and test set of 26,032.

Optimization We optimize the modulation parameters ϕ by stochastic gradient descent with Adam [17], an adaptive optimizer that normalizes the parameter updates by moving statistics of their norms. The learning rate is set to 0.001 with batch size 512 and cosine schedule. Optimization is performed for a single epoch for efficiency.

Baselines We evaluate a variety of baselines including domain adaptation, self-supervision, normalization, and confidence:

- source-only: the trained classifier is applied to the test set without adaptation.
- adversarial domain adaptation (RevGrad) [7]: reversing the gradients of a domain classifier optimizes the representation to be invariant to the source and target domains.
- self-supervised domain adaptation (UDA) [35]: joint optimization of self-supervised rotation and position tasks on the source and target encourages a shared representation.
- test-time training (TTT) [36]: the supervised model is augmented with an auxiliary task predictor, which shares its representation with the task model, and then both are jointly optimized during training. During testing, the auxiliary task is optimized further to update the shared representation. The specific auxiliary task for this method is rotation prediction [9].
- test-time normalization (batch norm): adaptive batch normalization [22] estimates separate mean and variance statistics on source data and target data. In our experiments, the mean and variance of all batch normalization layers are replaced with their estimates on the test/target data. These are the full estimates of the means and variances for the set, and not moving estimates.
- pseudo labeling (pseudo label) [21]: this approach defines a confidence threshold, assigns hard targets to any test prediction over the threshold, and then optimizes the model to these targets. This method indirectly reduces entropy, as hard targets have entropy zero, but is governed by the threshold hyperparameter. Our method directly minimizes entropy without such a hyperparameter.

The domain adaptation methods, RevGrad and UDA, do joint optimization over labeled source and unlabeled target data. Although TTT adapts at test-time, it first requires joint training on the source data to learn a representation compatible with the supervised and auxiliary task. Only test-time batch normalization, pseudo labeling, and our method are fully test-time adaptation methods.

3.1 Robustness to Corruptions

To benchmark robustness to corruption, we make use of common image corruptions [13], as computed offline for reproducibility. There are several corruption types, as detailed in our results tables, and each type has five severity levels from the least severe at one to the most severe at five. By default, we choose the most severe level, five, for all different types of corruptions in the following experiments. These corrupted test sets are CIFAR-10-C, CIFAR-100-C, and ImageNet-C.

We begin by illustrating the effect of our adaptation in Figure 3. Here we inspect the predicted classifications of three test points in CIFAR-10-C before and after adaptation. After entropy minimization over the entire test set, the adapted distributions have not only lower entropy but different peaks. This indicates that the shared modulation to minimize entropy results in different classifications, as is needed to correct errors.

	gauss	shot	impulse	defocus	glass	motion	zoom	snow	frost	fog	bright	contrast	elastic	pixelate	jpeg
CIFAR-10															
source-only	67.2	59.6	62.5	42.9	47.8	32.7	36.4	23.0	35.5	28.8	7.7	62.4	24.8	52.1	28.5
RevGrad	26.8	22.7	32.3	11.3	31.4	12.5	11.7	15.6	16.2	12.0	8.1	9.2	21.9	17.1	25.7
UDA	19.0	17.3	17.2	10.7	29.5	15.5	12.8	15.6	14.8	11.3	7.5	9.6	18.3	12.0	17.4
TTT	16.8	15.4	20.2	10.9	35.4	15.8	24.7	15.5	14.5	27.0	8.3	9.8	18.4	12.7	16.6
batch norm	25.4	22.1	32.6	10.7	31.2	10.8	9.9	14.0	14.1	11.0	6.2	10.0	18.5	17.7	25.5
pseudo label	22.0	20.2	29.3	10.4	31.5	11.0	9.0	12.8	14.8	10.3	7.8	10.7	19.8	14.0	21.6
minent (ours)	20.2	18.1	25.5	8.9	26.6	10.0	8.5	12.5	14.0	9.9	6.8	7.5	17.8	12.7	19.4
CIFAR-100															
source-only	89.9	88.1	95.1	65.6	81.4	55.6	59.0	53.0	65.9	59.1	31.9	77.8	51.4	76.5	57.6
RevGrad	49.9	47.6	57.1	29.3	51.8	31.2	28.6	37.0	37.7	34.3	25.8	27.1	40.8	34.8	50.0
UDA	54.3	51.9	46.1	35.8	59.1	44.5	40.4	45.0	42.2	41.3	31.1	37.4	46.3	36.7	47.6
TTT	47.7	46.0	50.3	34.4	63.3	41.7	47.4	42.6	44.9	61.9	31.2	36.4	43.8	36.5	47.0
batch norm	55.8	53.8	62.4	32.7	57.0	33.6	31.3	39.7	40.1	38.2	26.5	31.8	42.9	39.5	54.7
pseudo label	51.0	50.3	58.8	32.0	54.3	33.2	31.1	39.6	40.2	36.0	27.6	31.3	44.3	36.8	51.3
minent (ours)	46.8	45.4	53.3	29.4	49.9	30.5	28.6	36.4	36.6	32.7	26.3	26.8	40.6	33.7	45.8
ILSVRC															
source-only	94.2	92.9	93.9	84.2	91.7	87.8	77.2	84.5	77.9	79.6	42.5	95.4	84.0	71.7	61.3
batch norm	88.1	86.2	87.1	87.0	86.9	77.0	63.3	66.3	67.1	52.7	34.9	88.5	58.1	54.3	66.4
minent (ours)	74.3	70.1	71.4	74.2	75.2	58.2	49.5	49.8	61.3	40.6	31.7	81.5	43.7	40.8	47.4

Table 1: Corruption benchmark measuring percentage error on CIFAR-10, CIFAR-100, and ILSVRC following [13]. Image corruptions are applied only during testing to measure generalization. The baseline suffers a great drop in accuracy from its reference results on the uncorrupted test sets: 4.1% on CIFAR-10, 21.0% on CIFAR-100, and 23.5% on ILSVRC. Our method (minent) achieves the best accuracy in most cases while requiring less optimization than unsupervised domain adaptation methods and test-time training, which include joint training on source and target.

Next we verify that minimizing entropy with respect to the modulation parameters is in fact sufficient to reduce entropy. Figure 4 histograms the distribution of prediction entropy on the test sets of CIFAR-10-C, CIFAR-100-C, and ImageNet-C. The distribution before adaptation includes a larger range and a concentration of higher entropies, while the distribution after adaptation has a marginally smaller range and a marked concentration at lower entropies. (Note that the entropies on the original test sets, without corruption, are lower still. Our method has reached an intermediate degree of confidence.)

The full evaluation of the corruption benchmark is reported in Table 1. On the majority of corruptions and datasets our method achieves the lowest error. Notably many conditions have error rates in excess of 50% (see every condition on ILSVRC for example), even after adaptation by normalization, but our entropy minimization nevertheless reduces error.

The fifteen corruptions are arranged in columns, and the methods are arranged in rows, grouped by dataset. On CIFAR-10 and CIFAR-100 we compare all methods, including those that require joint training on source and target, given the convenient size of these datasets. On ILSVRC we compare the most efficient fully test-time methods—the source-only baseline, the normalization baseline, and our method—given the large-scale size of the training set at > 1 million images.

3.2 Target-Only Domain Adaptation

For unsupervised domain adaptation, we adopt the established setting of digit domain adaptation [7, 38, 39]. In particular we experiment with adaptation from SVHN to MNIST. The progress of our optimization is shown in Figure 5, and the resulting error rates are shown in Table 2. We verify that accuracy improves as entropy is reduced to justify our choice of objective. Our method achieves the lowest error across three architectures from a simple LeNet to a ResNet-26 in slimmer (W1) and wider (W4) editions.

Method	Data		Accuracy		
	Source	Target	LeNet	R-26(W1)	R-26(W4)
source-only	✓		19.5	18.2	16.8
RevGrad	✓	✓	17.1	12.2	12.6
UDA	✓	✓	24.4	14.4	12.4
batch norm		✓	18.9	15.7	15.4
pseudo label		✓	17.2	12.7	12.0
minent (ours)		✓	16.4	10.0	8.7

Table 2: Digit domain adaptation for SVHN \rightarrow MNIST. We compare the error rate of fully test-time entropy minimization against unsupervised domain adaptation methods, reverse gradient and self-supervised, plus fully test-time adaptation by batch normalization and pseudo-labeling. The low error of methods without source data shows the feasibility of target-only domain adaptation. Entropy minimization is the most accurate.

	source-only	single epoch			multiple epochs		
		ours (test)	ours (train)	oracle	ours (test)	ours (train)	oracle
LeNet	19.5	16.4	16.0	12.8	13.5	13.8	4.7
R-26(W1)	18.2	10.0	6.8	4.8	7.6	3.9	0.8
R-26(W4)	16.8	8.7	5.1	3.5	5.8	3.1	0.1

Table 3: Analysis results with more data, optimization, and supervision on SVHN \rightarrow MNIST. All results are error rates on the target test set.

3.3 Analysis

We provide sanity check, ablation, and oracle analysis experiments. As a sanity check, we evaluate our adaptation method on the original/clean test sets of the corruption benchmark. When the train and test data distributions are the same, and no adaptation is needed, our method does no harm. The accuracy of entropy minimization on the original test set is within 1% of the unadapted model. For ablation, we attempt to minimize entropy with respect to the model parameters θ . In every case this results in error rates worse than the baseline or no better. This negative result supports our optimization of modulation parameters.

For oracle analysis, we include more data, more optimization, and supervision in Table 3. We compare entropy minimization on target test, our method, with a variant on the larger target train, which significantly reduces error. Although we optimize for one epoch in our main experiments for efficiency, we experiment with multiple epochs (20 total) to gauge further improvement. Finally, to upper bound adaptation by modulation we optimize the cross-entropy given the target labels.

4 Related Work

We relate the fully test-time adaptation setting to existing adaptation settings, and highlight work that informs our approach of entropy minimization by affine modulation.

Adaptation Transfer learning, domain adaptation, and transduction adapt a model by extending its training given more data and supervision. Transfer learning by fine-tuning [5, 41] requires labeled target data for (re-)training the model. In our setting the target data is unlabeled, denying direct supervised learning of this kind. Domain adaptation [11] mitigates source/target differences by joint training on source and target. In unsupervised domain adaptation, the source data is labeled, but the target is not. This is closer to our setting, but still makes use of source data, while we have only target data. Transduction [6, 15, 43] fits predictions to a particular test set, in contrast to inductive methods that learn a general model for all test sets. Doing so requires joint computation over all of the training and testing points.

These approaches each have their purpose, but they do not cover all practical cases. How to adapt during testing, without any supervision, has received less attention. Inspired by these training-time

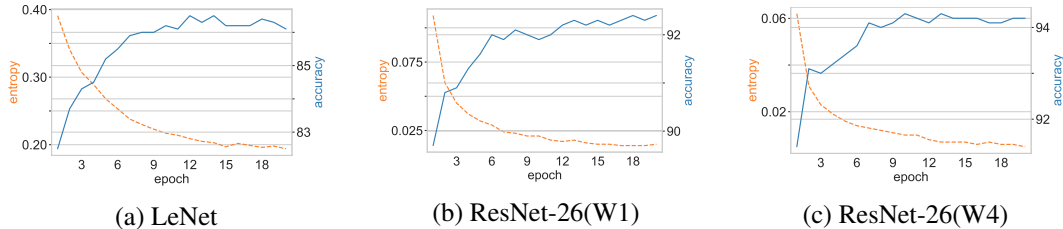


Figure 5: Optimization progress for digit classification on SVHN \rightarrow MNIST with three network architectures. We plot entropy and classification accuracy on the test set against the number of updates in epochs. The accuracy improves as entropy is reduced, justifying our choice of test-time objective.

adaptation approaches, we advocate for exploring test-time adaptation without reliance on source data and labels.

Entropy Minimization Entropy minimization is a key regularizer in semi-supervised learning and few-shot learning. These methods regularize a supervised objective by explicit or implicit entropy minimization during training. Their purpose is to prevent decision boundaries at high densities in the data distribution [10] and thereby improve accuracy for distinct class distributions.

Explicit methods optimize the sum of a supervised objective and entropy regularizer. Entropic semi-supervised learning [10] regularizes predictions on unlabeled training data, while entropic few-shot learning [3] regularizes predictions on the unlabeled test data. Implicit methods define targets for semi-supervised learning that reduce entropy without directly penalizing it. Pseudo-labeling [21] assigns hard labels to confident predictions on unlabeled data. A hard label is an indicator distribution over classes, for which the entropy is zero. MixMatch [1] sharpens target distributions for unlabeled data, where these target distributions are formed by averaging predictions over data augmentations. Optimizing a model on these hard or sharpened targets indirectly reduces entropy.

We apply entropy minimization to adapt a model during testing by unsupervised learning. Our experiments are the first to show the effectiveness of entropy as a standalone objective for adaptation.

Test-Time Optimization Recently, test-time training (TTT) by self-supervision [36] has been proposed to reduce generalization error. Self-supervision generates targets for auxiliary tasks that can be automatically labeled, such as recognizing rotations of an image. In TTT, the model is first jointly trained on the supervised task and an auxiliary task, and then the auxiliary task is further optimized at test-time. The test-time optimization can be episodic, over each test point independently, or online over all test points.

TTT and our test entropy method both optimize at test-time, but differ in their data requirements. Our method is fully test-time adaptation, without joint training on the source data, while TTT needs joint training. TTT depends on the choice of auxiliary task for supervision (indeed, [36] cautions that this task must be “both well-defined and non-trivial in the new domain”). Our test entropy objective is measured on the supervised task prediction, without an auxiliary task, and is in this way more domain-agnostic.

Feature Modulation Modulation is a form of conditioning that adjusts a model so that it varies with its input. Borrowing from its usage in signal processing, the modulation is usually simpler than the model, for example in being lower-dimensional than the model parameters. To simplify optimization, for robustness and speed, we optimize an adaptor to modulate the model instead of optimizing the model itself. We choose channel-wise affine transformation as an efficient and effective type of modulation that is used in batch normalization [14] and for conditioning features on the input [25] (in this role it is known as feature-wise linear modulation (FiLM) [25]). In these works on normalization and conditioning the modulation is optimized during training, as supervised by the task. We instead introduce modulation during testing, and optimize it by an unsupervised objective.

5 Conclusion

The main result of this work is that entropy can be a sufficient objective for fully-test time adaptation. This is remarkable in that this objective, while unsupervised, is purely a function of the supervised model training. In effect, it seems that the model has learned enough to supervise itself on shifted data. While there is still a notable gap in accuracy on corrupted data, and therefore further adaptation is needed, this is an encouraging step. Our fully test-time adaptation setting and experiments should encourage more exploration of what models may already know about the data distribution.

Broader Impact

As a work on unsupervised adaptation, it is our hope that this direction can make deep networks more accessible for pursuits with limited data and annotations. Not every group and purpose can afford the collection of massive training sets, much less labeling. In this way efficient methods to improve generalization might assist in the democratization of deep learning in smaller-scale contexts.

As adaptation research, our work inherits any benefits and disadvantages of the model that is adapted. To the extent that test-time entropy minimization reduces error, the cost of the failures of the adapted model will be reduced. With regard to biases in data, the goal of our optimization is to mitigate dataset shift. However, our technique attempts to maximize model certainty to do so, and may exploit over-represented features of the model training. Future work should investigate how fully test-time adaptation, and our test entropy minimization method, interact with training methods directed at calibration, robustness, and fairness.

Acknowledgments and Disclosure of Funding

We thank Eric Tzeng for discussions on domain adaptation, Bill Freeman for comments on the experiments, and Kelsey Allen for feedback on the exposition.

References

- [1] David Berthelot, Nicholas Carlini, Ian Goodfellow, Nicolas Papernot, Avital Oliver, and Colin A Raffel. Mixmatch: A holistic approach to semi-supervised learning. In *NeurIPS*, 2019.
- [2] Marius Cordts, Mohamed Omran, Sebastian Ramos, Timo Rehfeld, Markus Enzweiler, Rodrigo Benenson, Uwe Franke, Stefan Roth, and Bernt Schiele. The cityscapes dataset for semantic urban scene understanding. In *CVPR*, 2016.
- [3] Guneet Singh Dhillon, Pratik Chaudhari, Avinash Ravichandran, and Stefano Soatto. A baseline for few-shot image classification. In *ICLR*, 2020.
- [4] Carl Doersch, Abhinav Gupta, and Alexei A Efros. Unsupervised visual representation learning by context prediction. In *ICCV*, 2015.
- [5] J. Donahue, Y. Jia, O. Vinyals, J. Hoffman, N. Zhang, E. Tzeng, and T. Darrell. Decaf: A deep convolutional activation feature for generic visual recognition. In *ICML*, 2014.
- [6] A Gammernan, V Vovk, and V Vapnik. Learning by transduction. In *UAI*, 1998.
- [7] Yaroslav Ganin and Victor Lempitsky. Unsupervised domain adaptation by backpropagation. In *ICML*, 2015.
- [8] Robert Geirhos, Carlos RM Temme, Jonas Rauber, Heiko H Schütt, Matthias Bethge, and Felix A Wichmann. Generalisation in humans and deep neural networks. In *NeurIPS*, 2018.
- [9] Spyros Gidaris, Praveer Singh, and Nikos Komodakis. Unsupervised representation learning by predicting image rotations. In *ICLR*, 2018.
- [10] Yves Grandvalet and Yoshua Bengio. Semi-supervised learning by entropy minimization. In *NeurIPS*, 2005.
- [11] A. Gretton, AJ. Smola, J. Huang, M. Schmittfull, KM. Borgwardt, and B. Schölkopf. *Covariate shift and local learning by distribution matching*, pp. 131–160. MIT Press, Cambridge, MA, USA, 2009.

- [12] Kaiming He, Xiangyu Zhang, Shaoqing Ren, and Jian Sun. Deep residual learning for image recognition. In *CVPR*, June 2016.
- [13] Dan Hendrycks and Thomas Dietterich. Benchmarking neural network robustness to common corruptions and perturbations. In *ICLR*, 2019.
- [14] Sergey Ioffe and Christian Szegedy. Batch normalization: Accelerating deep network training by reducing internal covariate shift. In *ICML*, 2015.
- [15] Thorsten Joachims. Transductive inference for text classification using support vector machines. In *ICML*, 1999.
- [16] Alex Kendall and Yarin Gal. What uncertainties do we need in bayesian deep learning for computer vision? In *NeurIPS*, 2017.
- [17] Diederik Kingma and Jimmy Ba. Adam: A method for stochastic optimization. In *ICLR*, 2015.
- [18] A. Krizhevsky, I. Sutskever, and G. Hinton. Imagenet classification with deep convolutional neural networks. *NeurIPS*, 25, 2012.
- [19] Alex Krizhevsky. Learning multiple layers of features from tiny images. Technical report, University of Toronto, 2009.
- [20] Y. LeCun, L. Bottou, Y. Bengio, and P. Haffner. Gradient-based learning applied to document recognition. *Proceedings of the IEEE*, 86(11):2278–2324, 1998.
- [21] Dong-Hyun Lee. Pseudo-label: The simple and efficient semi-supervised learning method for deep neural networks. In *ICML Workshop on challenges in representation learning*, 2013.
- [22] Yanghao Li, Naiyan Wang, Jianping Shi, Xiaodi Hou, and Jiaying Liu. Adaptive batch normalization for practical domain adaptation. *Pattern Recognition*, 2018.
- [23] Yuval Netzer, Tao Wang, Adam Coates, Alessandro Bissacco, Bo Wu, and Andrew Y Ng. Reading digits in natural images with unsupervised feature learning. *NeurIPS Workshop on Deep Learning and Unsupervised Feature Learning*, 2011.
- [24] Adam Paszke, Sam Gross, Francisco Massa, Adam Lerer, James Bradbury, Gregory Chanan, Trevor Killeen, Zeming Lin, Natalia Gimelshein, Luca Antiga, et al. Pytorch: An imperative style, high-performance deep learning library. In *NeurIPS*, 2019.
- [25] Ethan Perez, Florian Strub, Harm De Vries, Vincent Dumoulin, and Aaron Courville. Film: Visual reasoning with a general conditioning layer. In *AAAI*, 2018.
- [26] Joaquin Quionero-Candela, Masashi Sugiyama, Anton Schwaighofer, and Neil D Lawrence. *Dataset shift in machine learning*. 2009.
- [27] Ilija Radosavovic, Justin Johnson, Saining Xie, Wan-Yen Lo, and Piotr Dollár. On network design spaces for visual recognition. In *ICCV*, 2019.
- [28] Ilija Radosavovic, Raj Prateek Kosaraju, Ross Girshick, Kaiming He, and Piotr Dollár. Designing network design spaces. In *CVPR*, 2020.
- [29] Benjamin Recht, Rebecca Roelofs, Ludwig Schmidt, and Vaishaal Shankar. Do ImageNet classifiers generalize to ImageNet? In *ICML*, 2019.
- [30] Stephan R Richter, Zeeshan Hayder, and Vladlen Koltun. Playing for benchmarks. In *ICCV*, 2017.
- [31] Olga Russakovsky, Jia Deng, Hao Su, Jonathan Krause, Sanjeev Satheesh, Sean Ma, Zhiheng Huang, Andrej Karpathy, Aditya Khosla, Michael Bernstein, et al. ImageNet large scale visual recognition challenge. *IJCV*, 2015.
- [32] C.E. Shannon. A mathematical theory of communication. *Bell system technical journal*, 27, 1948.
- [33] Evan Shelhamer, Jonathan Long, and Trevor Darrell. Fully convolutional networks for semantic segmentation. *PAMI*, 2017.
- [34] Karen Simonyan and Andrew Zisserman. Very deep convolutional networks for large-scale image recognition. In *ICLR*, 2015.

- [35] Yu Sun, Eric Tzeng, Trevor Darrell, and Alexei A Efros. Unsupervised domain adaptation through self-supervision. *arXiv preprint arXiv:1909.11825*, 2019.
- [36] Yu Sun, Xiaolong Wang, Zhuang Liu, John Miller, Alexei A Efros, and Moritz Hardt. Test-time training for out-of-distribution generalization. *arXiv preprint arXiv:1909.13231*, 2019.
- [37] Ajay Kumar Tanwani, Nitesh Mor, John Kubiawicz, Joseph E Gonzalez, and Ken Goldberg. A fog robotics approach to deep robot learning: Application to object recognition and grasp planning in surface decluttering. In *ICRA*, 2019.
- [38] Eric Tzeng, Judy Hoffman, Trevor Darrell, and Kate Saenko. Simultaneous deep transfer across domains and tasks. In *ICCV*, 2015.
- [39] Eric Tzeng, Judy Hoffman, Kate Saenko, and Trevor Darrell. Adversarial discriminative domain adaptation. In *CVPR*, 2017.
- [40] Jingdong Wang, Ke Sun, Tianheng Cheng, Borui Jiang, Chaorui Deng, Yang Zhao, Dong Liu, Yadong Mu, Mingkui Tan, Xinggang Wang, et al. Deep high-resolution representation learning for visual recognition. *PAMI*, 2020.
- [41] Jason Yosinski, Jeff Clune, Yoshua Bengio, and Hod Lipson. How transferable are features in deep neural networks? In *NeurIPS*, 2014.
- [42] Richard Zhang, Phillip Isola, and Alexei A Efros. Split-brain autoencoders: Unsupervised learning by cross-channel prediction. In *CVPR*, 2017.
- [43] Dengyong Zhou, Olivier Bousquet, Thomas Navin Lal, Jason Weston, and Bernhard Schölkopf. Learning with local and global consistency. *NeurIPS*, 2004.

Appendix

We report supplementary results for the method as described in Section 2. All of these results are collected with the *same method as-is*, with differences only in (1) the input and (2) the pre-trained model to be adapted.

A Robustness to Corruptions

In Section 3.1 we evaluate methods on a common image corruptions benchmark. In Table 1 we report results on the most severe level of corruption, level 5. In this appendix, we include examples of these image corruptions, and report results at milder levels of corruption for completeness.

Example Corruptions We summarize the image corruption types for the benchmark in Figure 6.

Varying Severity Error rates on milder corruptions for levels 1–4 are reported in Tables 4, 5, 6, and 7. The model and optimization details follow Section 3.1, and only the level of input corruption differs.

	gauss	shot	impulse	defocus	glass	motion	zoom	snow	frost	fog	bright	contrast	elastic	pixelate	jpeg
CIFAR-10															
source-only	21.1	13.3	14.6	4.4	42.9	9.0	11.6	8.3	8.7	4.4	4.2	4.7	8.6	5.9	12.3
TTT	9.8	8.1	8.6	7.1	24.8	9.8	16.1	10.1	8.3	7.0	6.7	7.1	10.0	8.0	11.1
batch norm	9.4	7.1	8.9	4.0	21.5	5.5	5.9	7.2	6.3	4.3	4.0	4.2	7.0	5.5	10.9
pseudo label	9.1	7.7	8.7	5.1	19.7	6.5	7.4	6.8	7.5	5.7	5.2	5.1	8.4	6.5	11.7
minent (ours)	8.7	7.0	8.7	4.6	17.0	6.1	6.3	7.0	7.0	4.7	4.9	4.8	7.5	6.2	10.2
CIFAR-100															
source-only	56.6	44.4	44.6	21.5	79.2	30.5	33.8	30.0	32.9	21.9	21.4	22.3	29.5	25.7	37.9
TTT	34.3	31.3	31.0	26.8	52.9	31.4	35.9	33.2	31.3	27.9	27.4	27.7	33.5	29.7	35.8
batch norm	32.6	28.8	30.8	21.0	45.5	24.4	23.5	26.6	26.3	21.2	21.2	21.1	26.2	23.9	35.7
pseudo label	32.6	30.0	31.1	22.4	43.3	25.9	24.3	27.3	27.2	23.6	22.3	22.6	27.2	26.0	34.4
minent (ours)	29.6	27.4	28.6	21.6	39.7	24.3	23.1	25.9	26.3	21.8	21.9	21.9	26.9	24.0	31.7
ILSVRC															
source-only	37.5	38.5	47.0	41.1	44.6	35.8	46.8	46.8	39.8	40.2	27.1	35.8	32.8	32.7	33.8
batch norm	35.1	35.9	40.8	41.3	38.5	32.5	39.2	38.4	35.6	31.2	25.4	29.1	29.7	28.9	32.4
minent (ours)	31.3	31.7	34.9	33.8	32.2	29.6	34.2	33.0	32.9	29.1	25.4	27.6	28.6	27.5	29.9

Table 4: Corruption benchmark measuring percentage error on CIFAR-10, CIFAR-100, and ILSVRC at severity level 1 (least severe).

	gauss	shot	impulse	defocus	glass	motion	zoom	snow	frost	fog	bright	contrast	elastic	pixelate	jpeg
CIFAR-10															
source-only	40.6	22.7	27.0	5.7	41.4	15.5	14.7	18.7	13.9	5.5	4.4	7.8	8.9	10.2	18.3
TTT	12.2	9.9	11.0	6.8	25.6	11.1	16.0	13.0	10.4	7.6	7.1	7.5	10.7	8.3	13.4
batch norm	13.2	9.1	13.1	4.2	21.1	6.8	5.8	11.5	8.2	4.6	4.3	5.1	6.6	6.6	16.9
pseudo label	13.2	9.0	12.1	5.0	19.1	7.6	6.6	10.9	9.3	6.2	5.4	6.7	8.0	7.8	18.4
minent (ours)	11.2	9.2	11.5	4.9	16.0	7.2	6.2	9.3	8.5	5.2	5.1	5.3	7.3	6.7	14.1
CIFAR-100															
source-only	74.8	57.9	67.1	25.1	78.8	39.1	38.6	47.7	42.6	25.2	22.0	28.7	30.0	33.2	46.6
TTT	38.9	34.6	34.7	27.4	50.9	34.3	37.8	36.9	35.6	28.7	28.1	29.4	33.9	30.9	40.8
batch norm	40.8	34.0	38.6	21.3	46.5	26.9	24.1	34.6	30.6	22.5	21.5	22.4	25.3	25.4	43.6
pseudo label	38.4	32.3	36.8	22.8	44.2	27.3	25.2	33.1	31.4	23.6	23.0	23.4	27.2	26.6	40.1
minent (ours)	35.7	30.4	34.0	22.0	39.6	26.3	23.6	31.3	29.7	22.6	22.1	22.7	26.3	25.2	37.7
ILSVRC															
source-only	47.6	50.7	57.0	48.3	59.6	46.6	56.7	69.6	57.3	47.0	28.8	42.3	54.6	35.4	36.9
batch norm	44.1	46.3	50.6	51.6	51.4	41.0	46.3	53.0	49.5	34.3	26.4	32.1	45.7	30.4	36.9
minent (ours)	36.4	36.9	40.6	39.2	39.0	33.6	38.2	41.4	42.1	30.5	26.2	29.3	40.9	28.1	32.3

Table 5: Corruption benchmark measuring percentage error on CIFAR-10, CIFAR-100, and ILSVRC at severity level 2.

	gauss	shot	impulse	defocus	glass	motion	zoom	snow	frost	fog	bright	contrast	elastic	pixelate	jpeg
CIFAR-10															
source-only	56.9	42.2	36.6	10.6	38.9	24.1	20.5	14.5	23.0	7.2	5.0	11.3	13.1	14.7	20.5
TTT	14.9	12.1	13.7	7.0	24.5	13.7	16.3	13.9	12.1	9.3	7.6	7.5	10.9	8.8	13.9
batch norm	19.6	15.2	17.8	4.7	20.6	9.0	6.7	11.5	10.9	5.2	4.6	5.5	7.4	7.8	18.4
pseudo label	17.0	15.8	16.0	5.6	18.3	9.2	6.8	11.5	11.2	6.9	6.1	5.7	8.1	8.7	16.3
minent (ours)	15.6	12.6	14.7	5.6	15.6	8.9	6.7	11.3	10.6	5.7	4.9	5.9	7.8	7.7	15.9
CIFAR-100															
source-only	84.4	77.5	79.9	34.8	74.8	48.3	45.3	41.4	54.7	29.0	23.3	35.3	36.8	39.8	49.2
TTT	43.9	39.4	37.5	28.6	53.3	37.2	41.9	38.6	40.0	36.6	28.4	30.1	35.8	31.4	42.2
batch norm	48.5	44.4	44.1	22.2	46.6	30.8	25.7	34.3	35.2	24.2	22.2	23.7	26.9	27.2	46.8
pseudo label	46.2	41.6	41.4	23.1	43.3	30.1	26.1	34.0	36.2	25.2	23.5	24.1	28.6	27.8	43.3
minent (ours)	40.7	36.9	38.6	22.4	39.4	29.1	24.8	32.3	33.0	24.0	22.8	23.2	26.8	26.7	39.8
ILSVRC															
source-only	64.2	66.5	65.6	63.6	83.0	65.4	64.8	66.4	69.1	56.6	31.5	55.2	45.9	46.3	39.6
batch norm	58.3	59.2	58.9	68.7	71.3	54.8	52.1	52.9	59.3	38.9	28.0	38.7	35.0	37.0	40.8
minent (ours)	44.5	44.4	45.0	50.8	52.8	40.1	41.6	41.1	50.1	32.7	27.5	32.0	30.2	31.6	34.2

Table 6: Corruption benchmark measuring percentage error on CIFAR-10, CIFAR-100, and ILSVRC at severity level 3.

	gauss	shot	impulse	defocus	glass	motion	zoom	snow	frost	fog	bright	contrast	elastic	pixelate	jpeg
CIFAR-10															
source-only	63.2	48.5	49.9	19.7	50.8	23.9	26.4	17.2	25.2	10.9	5.7	20.4	20.0	31.9	23.5
TTT	16.1	14.2	16.5	8.6	37.0	13.4	17.2	15.9	12.6	14.0	7.7	8.5	14.2	10.1	15.4
batch norm	23.1	17.7	25.8	6.4	31.1	8.7	7.6	12.8	11.4	6.2	5.0	6.4	11.7	10.9	20.8
pseudo label	23.1	15.6	25.8	7.5	30.5	8.4	8.0	12.3	11.8	7.5	6.4	7.4	13.3	10.0	17.9
minent (ours)	18.2	14.0	20.7	6.8	24.6	8.7	7.2	12.0	10.7	6.7	5.6	6.0	11.9	9.0	17.1
CIFAR-100															
source-only	87.4	82.8	91.4	46.9	84.7	48.0	51.4	44.4	56.1	36.2	25.5	46.8	44.3	60.1	53.0
TTT	46.1	42.3	43.9	31.1	62.7	36.7	43.8	40.6	39.4	48.3	29.2	31.3	39.8	32.9	43.3
batch norm	51.6	47.3	54.4	25.3	57.5	30.0	28.0	36.6	35.7	28.1	23.4	25.3	34.4	31.7	50.3
pseudo label	48.0	43.8	50.0	26.0	56.3	30.3	29.3	37.9	35.2	28.5	24.7	26.1	35.1	30.9	47.0
minent (ours)	44.4	40.0	46.1	24.5	50.1	28.4	26.3	34.5	33.1	27.4	23.9	24.1	33.2	28.8	41.7
ILSVRC															
source-only	81.8	85.7	83.2	75.5	87.9	81.0	71.3	77.9	71.1	63.7	36.1	81.1	58.8	61.6	48.3
batch norm	73.5	76.9	75.0	79.5	78.4	69.2	58.2	63.5	60.8	42.3	30.9	61.5	41.3	47.9	52.9
minent (ours)	55.5	58.0	56.7	62.0	60.9	50.2	45.4	47.9	51.7	34.9	29.3	41.0	33.2	36.9	39.6

Table 7: Corruption benchmark measuring percentage error on CIFAR-10, CIFAR-100, and ILSVRC following [13] at severity level 4.

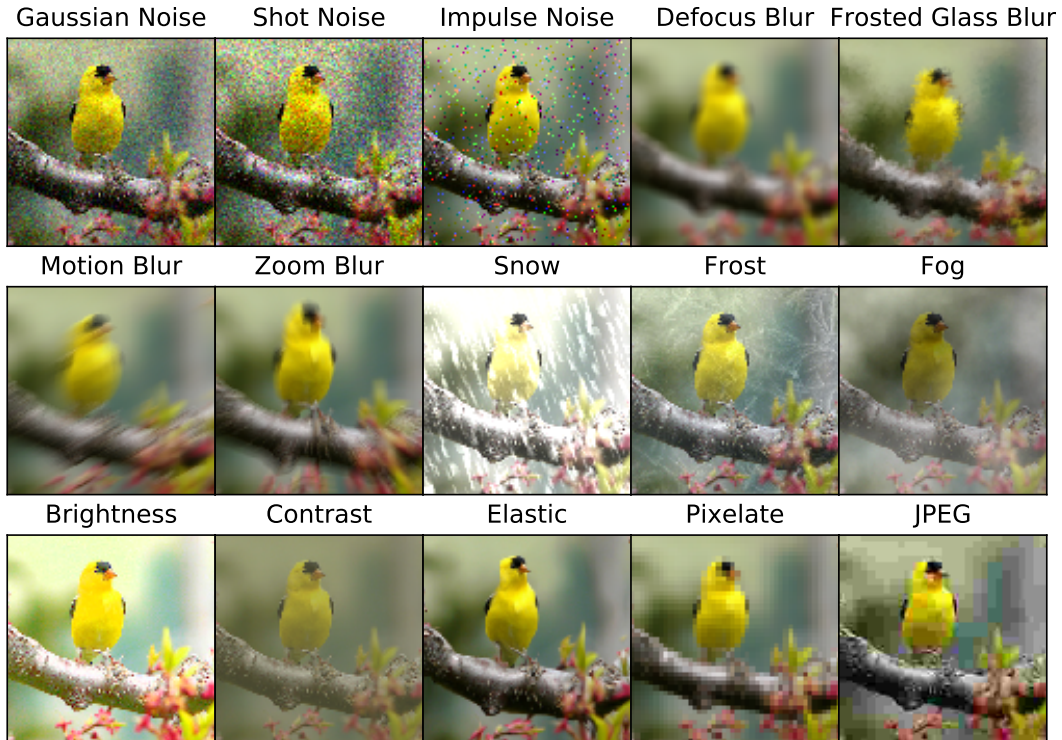


Figure 6: Examples of each corruption type in the image corruptions benchmark. (Figure reproduced from [13]).

B Target-only Domain Adaptation

In Section 3.2 we evaluate methods for digit domain adaptation. We focus on target-only domain adaptation in our fully test-time adaptation setting. In Table 2 we quantitatively compare unsupervised domain adaptation with our method and baselines. In this supplement, we include a qualitative result for target-only domain adaptation for semantic segmentation (pixel-wise classification) with a simulation-to-real (sim-to-real) domain shift.

For the sim-to-real condition, the source data is simulated while the target data is real. Our source data is GTA [30], a visually-sophisticated video game set in an urban environment, and our target data is Cityscapes [2], an urban autonomous driving dataset. The supervised model is HRnet-W18, a fully convolutional network [33] in the high-resolution network family [40]. We minimize entropy over a single input image, because an image is effectively a dataset of pixels. This is a direct analogy of the classification task experiments in the main text.

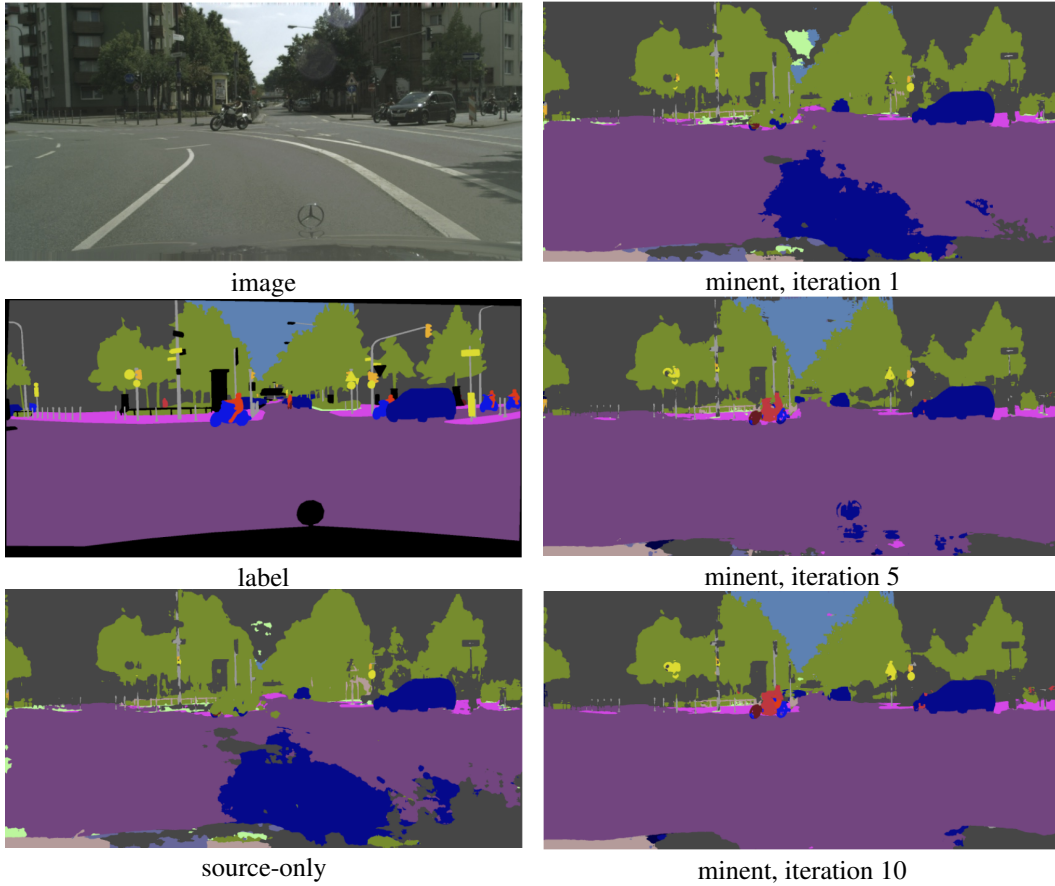


Figure 7: Domain adaptation on a semantic segmentation task with simulation-to-real shift from GTA [30] to Cityscapes [2]. Our fully test-time adaptation by entropy minimization only uses the target data, and optimizes over a single image as a dataset of pixel-wise predictions. In only 10 iterations our method suppresses noise (see the completion of the street segment, in purple) and recovers missing classes (see the motorcycle and rider, center).